International Journal of Systems Signal Control and Engineering Application 9 (3-4): 86-96, 2016
ISSN: 1997-5422

Effect of Zn Interlayer on Microstructure and Mechanical Properties of Dissimilar Al/Mg Weld by FSW

[1]Majid Shirinabadi Farahani and [2]Mehdi Divandari
[1]Department of Materials, Islamic Azad University, South Tehran Branch, Tehran, Iran
[2]School of Materials and Metallurgy Engineering, Science and Technology University, Tehran, Iran

Abstract: In this research, the effect of interlayer thickness of pure Zn on pure Al and Mg joint with lap joint form of welded top Mg with FSW welding process was investigate. The assumption considered: tool rotation speed 1600 rpm, welding speed was 40 mm min^{-1} and all of weld parameters was constant, pure Zn interlayer with three thickness were 400, 200 and 100 μ, respectively. Welded specimens were examined microscopically (optical microscope, SEM, EDS) and macroscopically and XRD processes. Microstructure analysis shown that complex structure composed of Al and Mg layer was obtained in the interface of joint and Mg-Al-Zn solidified and eutectic structures are visible. There is $MgZn_2$ intermetallic compound in the Mg and Zn interface and weld zone. The weld shear tensile strength has increase by reduction of Zn interlayer thickness. The maximum weld shear tensile strength with interlayer pure Zn thickness 100 μ was 76 N mm^{-2}. The weld zone micro hardness was much more than two base metals.

Key words: Friction stir welding, aluminum, magnesium, Zn interlayer, intermetallic compound

INTRODUCTION

Friction Stir Welding (FSW): In compare to the other methods of welding, FSW is a new one. As, welding of dissimilar metals by fusion methods causes different kinds of problems, solid-state methods are recommended. After constant rotation, welding tools will stop for a few seconds and then move forward. As a result, pulp materials around the tool will be dragged to the mixing area. During this process, the turbulence and heat in the weld zone will cause changes in the distribution of impurities and the size of knurls around and center of joint zone (Elyasi *et al*., 2015; Elias *et al*., 2015; Mishrar and Ma, 2005).

Welding of Al and Mg as light industrial alloys are of great importance in structures related to Aviation and aerospace industry. Researchers have suggested different process of dissimilar Al/Mg welding till now (Chen and Nakata, 2008). In Al/Mg fusion welding, the joint is very frail, because of the formation of thick and contiguous layer intermetallic compound in the interface of joint (Liu and Liu, 2006). Considering the recent researches, lap joint form of welding of Al/Mg by FSW was first observed in 2003 (Mclean *et al*., 2003). Till 2015, some other researchers have examined the joint between different alloys of Al/Mg. The results show that the formation of weak intermetallic compound within the interface of Al/Mg joint has negative effect on the strength and flexibility of joint (Kostka *et al*., 2009; Firouzdor and Kou, 2010).

Less attention has been paid to the lap joint form of Al/Mg welding with interlayer in FSW. This method has been remained just as a suggestion within which the application of Zn is recommended. In 2010, the effect of ceramic powders as an interlayer in FWS was raised in patent (Szymanski *et al*., 2010). In other research in 2012, the interlayer effect of Sn/Cu alloy in FSW was investigated which results show a tangible increase in the weld tensile strength in different rotation speeds (Venkateswaran and Reynolds, 2012).

Although, no research has been done regarding the interlayer effect of Zn on the simple system of Al/Mg, its effect on the intrusive joint of Al 6061 to Mg AZ31B has been examined. The application of Zn interlayer prevents the formation of frail and contiguous intermetallic compound. In the presence of Zn interlayer, the intermetallic compound will be formed as dispersed particles within the thin layer of joint-interface with a thickness of 1 μ. Zn interlayer will increase the weld tensile strength approximately, 2 time from 31.4-75 MPa

Corresponding Author: Majid Shirinabadi Farahani, Department of Materials, Islamic Azad University, South Tehran Branch, Tehran, Iran

(Zhao and Zhang, 2008; Liu *et al*., 2009). Also, a successful research has been done regarding the Gas Tungsten Arc Welding (GTAW) of Al 6061 Mg AZ31B by applying an arc welding process that uses a non-consumable tungsten electrode to produce the weld (Liu *et al*., 2012, 2013). In 2011, an experiment done on the MAG welding of Al/Mg with Zn interlayer within which the eutectic structures of temperature was observed low and weld strength with interlayer was increased (Zhang and Song, 2011). Also in 2015, an investigation has been done on the welding of Al/Mg with Zn interlayer by the process of resistance spot welding.

MATERIALS AND METHODS

Experimental procedures: In this research, pure Al and Mg sheets were used. Both sheets sizes were 3×65×100 mm. Zn sheets were 30×100 mm with three thickness of 100, 200 and 400 μ which were cleaned by Acetone. The chemical composition of the sheets are listed in Table 1-3. The tools used in this research are of hot research tool steel H_{13} with triangle-shaped pins. The chemical composition of tools are mentioned in Table 4.

Welding experiments were done with the semi-automatic angle-grinder on the dynamic table made by Tabriz Machinery Manufacturing Co. Adjusting and integration of exerted vertical force was measured by the level of penetration of the tool shoulder into the top sheet. The penetration level for all the dissimilar welding specimens were considered 0.1 mm. The deviation angle of the tools for all the experiments were 3°C. Pin height was 2.6 mm and welding was done in a constant form. During the processes, the Mg sheet was on top and the Al was under it. Figure 1 and 2 show the placement of sheets in the fixture and schematic of the used tool.

In all cases, tool rotation speed was 1600 rpm and welding speed was 40 mm min^{-1}. Interlayer Zn with three thickness of 100, 200 and 400 μ were used for welding. Welding done, metallography specimens were prepared from three different welding zone, polished and engraved within four phases. It was done because of investigating the microstructure of welding specimens from the perpendicular section of stir zone (mixing area). Within first phase, the specimens were engraved with a solution with 10 mL acetic acid, 10 mL distilled water and 6g picric acid in 100 mL ethanol for 10 sec in order to detect the presence of Mg. Within the second phase, specimens were engraved with a solution of 20g of NaOH in 100 mL

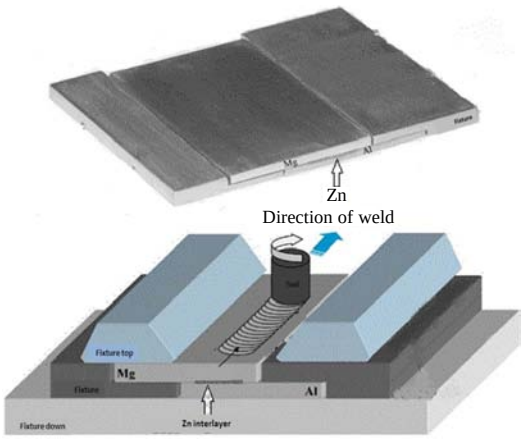

Fig. 1: Image and schematic of sheets and tools placement

Fig. 2: Schematic and Image of beveled triangle-shaped pin

Table 1: Chemical composition of Al sheet

Elements	Al	Si	Fe	Zn	Mg	Ni	Pb
Percentage	Rest	0.07	0.335	0.012	0.053	0.023	0.027

Table 2: Chemical composition of Mg sheet

Elements	Mg	Al	Cu	Fe	Mn	Si	Zn
Percentage	Rest	0.056	0.018	0.002	0.033	0.024	0.13

Table 3: Chemical composition of Zn sheet

Elements	Zn	Sn	Sb	Pb	Cd	Mg	Ni
Percentage	99.47	0.2	0.05	0.004	0.004	0.2	0.02

Table 4: Chemical composition of welding tools

Elements	C	Cr	Mo	Si	V	Mn
Percentage	0.39	4.95	1.13	0.96	0.95	0.4

distilled water for 40 sec to detect knurl. Third phase encompassed engraving the specimens with a solution of 4gr $KMnO_4$ and 2 g of NaoH in 100 mL of distilled water for 25 sec in order to coloring Al, Mg and intermetallic compound into different colors. At last, in order to investigate the Zn zone, a solution of 2ml of HF and 5 mL HNO_3 and water was used (Liu *et al*., 2007; Figaad *et al*., 2001; Elyasi *et al*., 2015; Nandan *et al*., 2006; Firouzdor and Kou, 2009). Optical microscope was used to detect from micro to magnifying 1000. SEM with EDS 30 KV was used for measuring the chemical composition. Also, X-ray diffraction was used to identify intermetallic compounds.

RESULTS AND DISCUSSION

Zn interlayer effect with a thickness of 400 μ: In Fig. 3, the image-result of SEM from the welding zone with 400 μ interlayer has been figured. This image shows that within the joint zone there exist different areas that distinguish in case of general mixing conditions (including zones 1-3; Fig. 3b-d). It is observed that because of difference in the density of Al, Mg and Zn and formation of phases, the level of brightness and darkness in the resulted image from SEM are variable. Table 5 indicates data elicited from the element analysis of related zones. Besides these three zones, a zone can be seen with 3 mm length and a thickness of 300-400 mm in the bottom of the image and in the interface of stir zone and Al sheet. This zone is marked with black holes in the image. These holes are considered as serious imperfections of this joint. Considering the conditions under which the experiment has been done (number of rotations, speed and 400 μ-interlayer), there is doubt to have access to the intact particle. So, investigating the structures of this zone is of great importance.

Figure 3c and d shows the SEM result from the zone 1 of Fig. 3. Table 5 indicates the element analysis of the respective zones. Based on the point to point element analysis, point A is full of Al, point B is near to the zone of Al/Mg/Zn solid solution in 3-phase diagram. Point C is the complete solid solution of Al/Zn which in together can be solved. It is likely that in point D, within the 3-phase diagram, we can observe Mg/Zn intermetallic compound. Also, because of proximity to the Mg zone, there is a possibility of the formation of $MgZn_2$ intermetallic compound (Zhao and Zhang, 2008; Liu *et al*., 2009). Figure 4 and 5 show the 3-phase diagram of Al/Mg/Zn and 2-phase diagram of Mg/Zn, respectively. Point E indicates interface of stir zone and the zone which is rich in Mg. If we pay attention to the 3-phase diagram, the lowest temperature in which triple phases are formed is 360°C.

Figure 3c shows magnifying of zone 2. Results from the element analysis of points F, G, H shown in Table 5, indicate that the structure of zone 2 in Fig. 3 contain very low concentration of Al. Also, eutectic structure is observed in zone H, considering atomic percent and 3 phase diagram. Point H is similar to the eutectic structures reported by the others (Zhang *et al*., 2015). In points G, F three elements of Al/Mg/Zn were observed but the density of Al was so low between 3-6%. Based on the 3-phase diagram of these elements and reported atomic percent in the element analysis, these two points are placed in an area within the 3-phase diagram which $MgZn_2$ intermetallic compound is likely to be constant (Zhang and Song, 2011; Zhang *et al*., 2015) (Fig. 4 and 5).

Figure 3d shows a magnifying of zone 3 which has a structure with high density Mg and Zn. It has to be mentioned that Mg density is higher. In this zone, the compounds are a subordinate of 3-phase diagram. Within the points under the names of J, K, L, the three elements of Al, Mg and Zn can be observed. After mixing, based on the 3-phase diagram and reported atomic percent in the EDS element analysis, these points are placed in the zone which the eutectic compound of Al Mg Zn and solid solution are constant. The factor to be noted is the underrepresentation of Al in the stir zone. It might be as the result of higher thickness of Zn interlayers which can cause the formation of intermetallic compound. Point J has a similar condition. Based on element analysis shown in Table 5 and by investigating 3-phase diagram, $MgZn_2$ is likely to be observed.

Results from the XRD of welding zone specified the presence of $MgZn_2$ intermetallic compound in interface of joint. Figure 6 shows XRD result of the specimens with 400 μ-interlayer.

Zn interlayer effect with thickness of 200 μ: Here, without superficial imperfection, welding area has a good quality and in the microscopic image, there is no trace of holes and discontinuity. As it is seen in the image, stir zone and different phases can be observed clearly with the variable levels of brightness and darkness. By this investigation, formed structures are of high importance in this zone which is essential to be elaborated in this study. SEM image of the welding zone with the interlayer of 200 μ and selected zones for EDS element analysis can be seen in Fig. 7.

Zone 1 is the stir zone. The magnifying of this zone has been shown in Fig. 7b. By investigating this

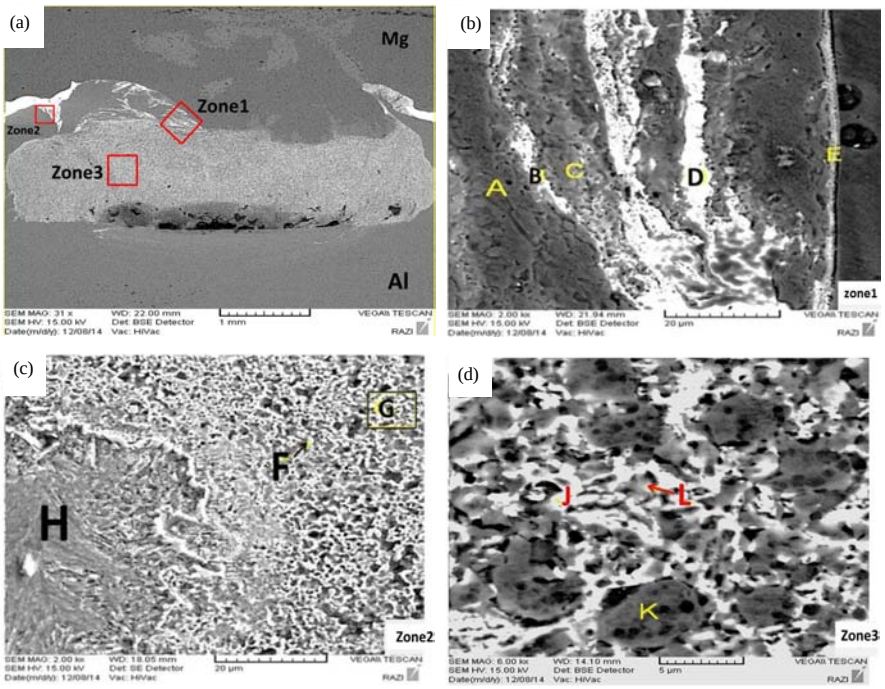

Fig. 3: a) The general image of the SEM from the welding zone and analyzed area of specimens with 400 µ-interlayer; b) Magnifying of zone 1 and analyzing points A-E; c) Magnifying of zone 2 and analyzing points F-H same and d) Magnifying of zone 3 and analyzing points L-J-K

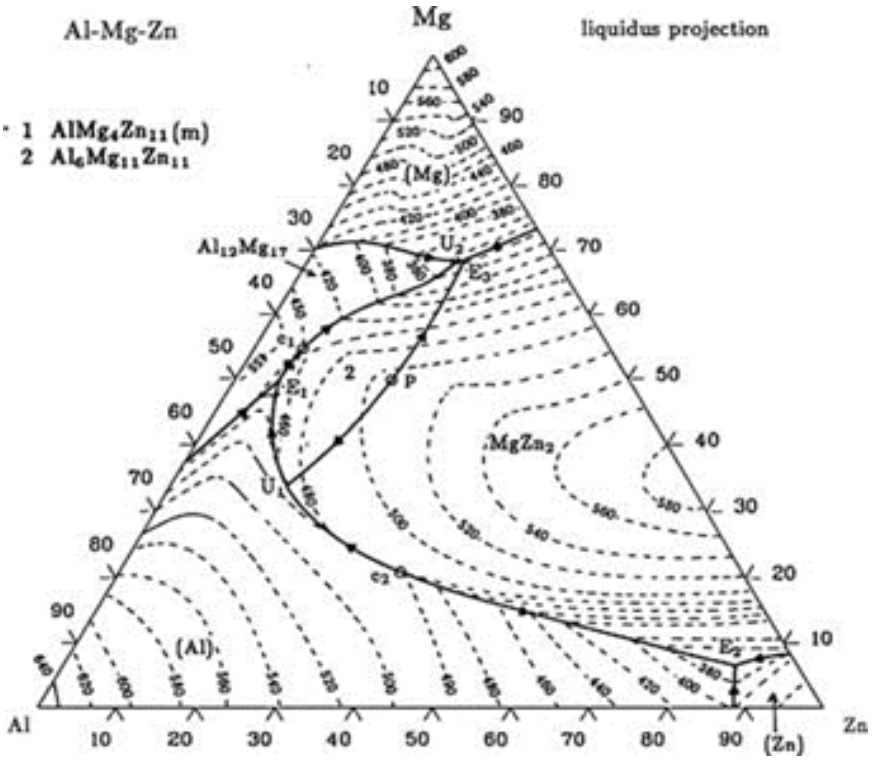

Fig. 4: Three phases (Al/Mg/Zn) diagram

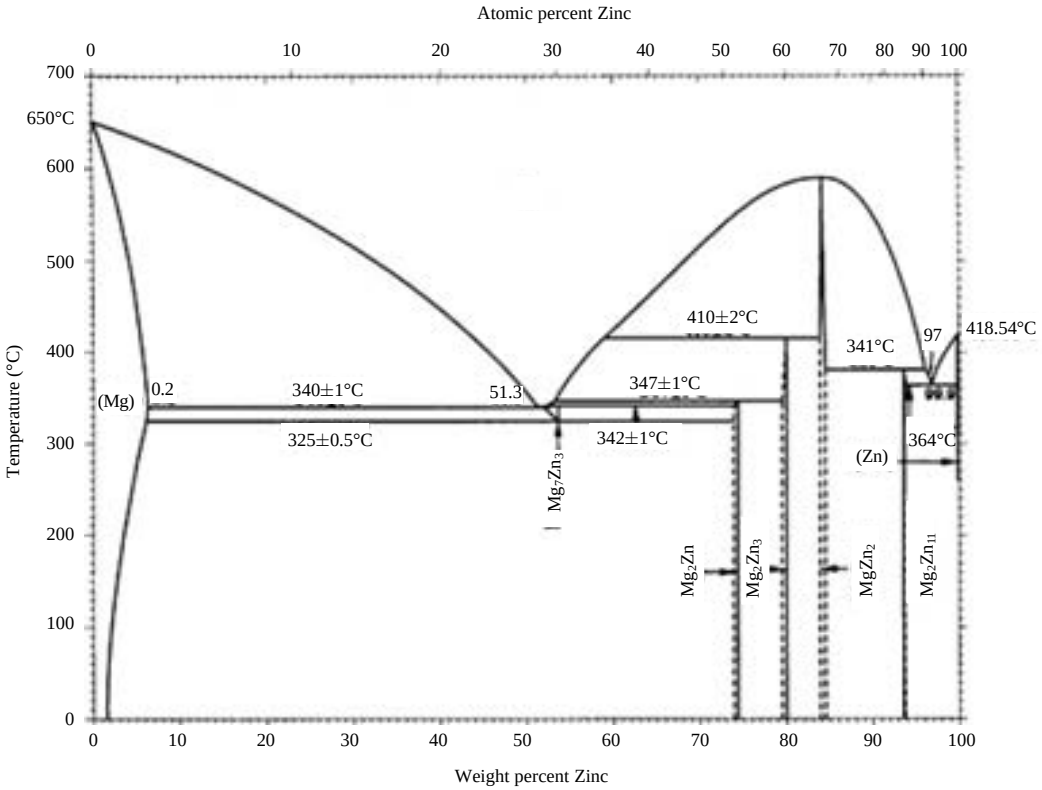

Fig. 5: Two phases (Mg/Zn) diagram

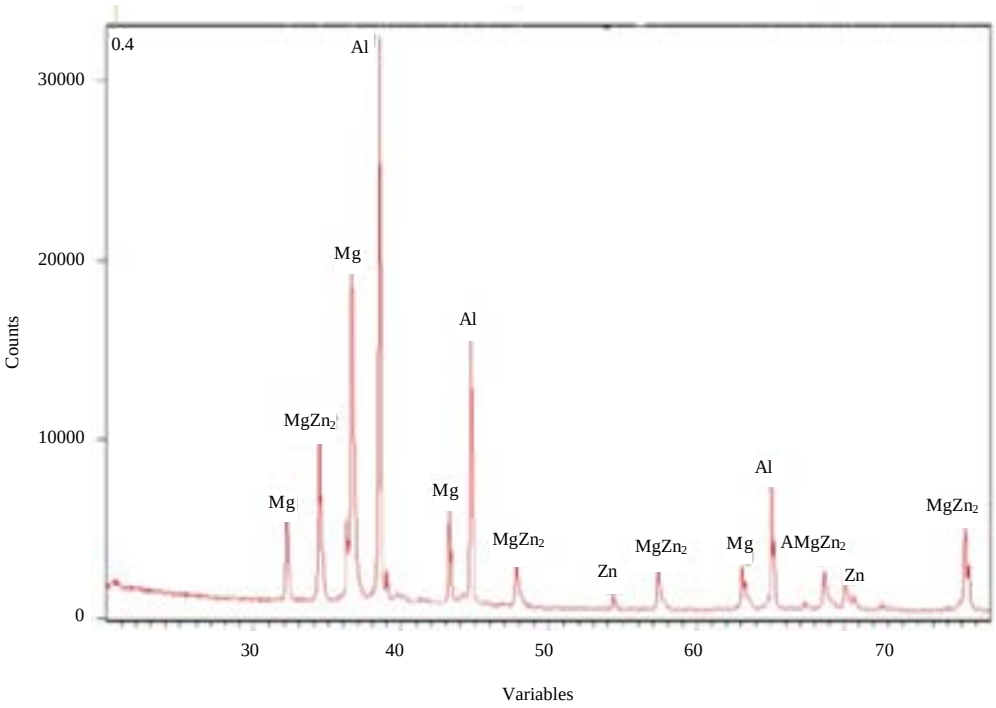

Fig. 6: XRD from joint area with 400 μ-interlayer

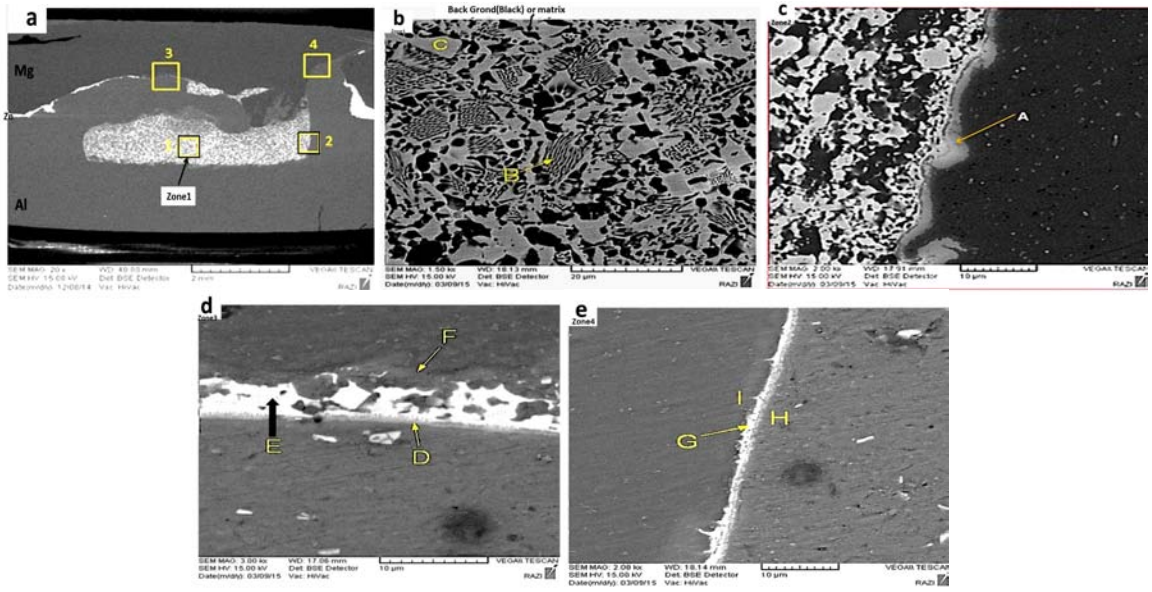

Fig. 7: a) SEM image of welding zone and analyzed area with 200 μ-interlayer; b) Magnifying of zone 1 in image 7-a and point-to-point element analysis areas; c) Magnifying of zone 2; d) Magnifying of zone 3 and details; e) Magnifying of zone 4 and related details

Table 5: Element analysis of zone 1-3 welding with 400 μ thickness interlayer

Test zones/focus point of the microscope	Al atomic (%)	Mg atomic (%)	Zn atomic (%)
Zone 1			
A	98.54	0.260	1.200
B	52.17	15.32	32.51
C	9078	0.850	8.370
D	15.25	31.47	53.26
E	54.90	41.26	3.730
Zone 2			
F	5.900	38.98	55.13
G	6.390	38.28	56.34
H	3.280	73.10	23.63
Zone 3			
L	14.48	7.550	55.13
J	25.30	15.70	58.98
K	5.900	3.840	90.97

Table 6: Element analysis of zones 1-4 welding with 200 μ-interlayer

Test zones/focus point of the microscope	Al atomic (%)	Mg atomic (%)	Zn atomic (%)
Zone 1			
Background (black)	6.700	86.55	6.700
B	18.80	67.83	13.31
C	2400	61.75	14.20
Zone 2			
A	62.08	28.09	9.840
Zone 3			
D	81.51	15.51	2.980
E	23.94	56.40	19.64
F	11.41	69.11	18.97
Zone 4			
H	72.06	22.32	5.620
G	29.28	50.14	20.57
I	4.730	9280	2.470

area and assessing element analysis (Table 6), Al underrepresentation is clear and in the field point it is approximately equal to 6%. So, the element amount of Zn in some points of welding zone is in balance with Al. So, this issue can results in the higher risk of the intermetallic compound presence. Considering the EDS element analysis shown in Table 6 and by investigating these points in the 3-phase diagram, it is likely to observe solid solution of Mg and triad eutectic compounds in the areas full of holes with in point B. These full of holes areas are very similar to images of the (Liu *et al*., 2013; Zhang *et al*., 2015).

Zone 2 on Fig. 7d shows there is a risk of intermetallic compound presence mentioned in the reference (Firouzdor and Kou, 2010). But after point-to-point analysis indicated in Table 6 and comparing it with the 3-phase diagram, the existence of intermetallic compound is less likely to be happen. By studying zone 3 element analysis shown in Table 6 and matching it with 3-phase diagram, it is clear that point E is the interface point inclined toward Mg and it is likely to observe constant $MgZn_2$ there. Point D is placed within the 2 and 3 phase diagram in the solid solution point of Al/Mg. Within the 3-phase diagram, element analysis of point F is placed in the zone of solid solution while the density of Mg is higher. Figure 7d shows the magnifying of zone 3 and element analysis points of D, E and F.

Studying element analysis shown in Table 6 and matching it with the 3-phase diagram, it can be concluded that point G in Figure 7e is a point in the interface inclined toward Mg within which constant $MgZn_2$ is likely to be seen. Point H is toward Al and point I is close to Mg. By observing their atomic percent in Table 6, it is clear that the risk of intermetallic compound presence is lower and the compound of this point is toward solid solution. Results from XRD of 200 μ-interlayer show that there exists $MgZn_2$ in welding zone and the interface. Yet, we observe a low density of Al. Figure 8 shows the result of XRD for a specimens with 200 μ interlayer.

Zn interlayer effect with a thickness of 100 μ: In specimens with 100 μ-interlayer, welding zone is of high quality and without superficial imperfections. In the microscopic image, there is no trace of holes and discontinuity. So, it shows that welding variable are chosen properly. Figure 9 indicates welding zone and selected areas for EDS element analysis for a specimen of 100 μ-interlayer. By decreasing the thickness to 100 μ, the density of Zn will be lessen and the Al will be increased. Considering the 3-phase diagram, an increase in the density of Al will lessen the risk of the intermetallic compound presence. And vice versa as Zn is increasing, in the presence of Mg and low density of Al, constant $MgZn_2$ will be formed within the 3-phase diagram (Venkateswaran and Reynolds, 2012; Zhang *et al*., 2015).

Figure 9b shows magnifying of zone 1, e.g., interface near stir zone. This zone is mentioned as a possible one for the existence of intermetallic compounds (Firouzdor and Kou, 2010). In a 100 μ specimen, considering the percentage resulted from interface by EDS point analysis (Table 7), there is a possibility of Al/Mg solid solution and eutectic compound of these elements. Assessments show there is no trace of intermetallic compound. So, this a good news for the 100 μ-specimen which surely affect the welding quality positively (Chen and Nakata, 2008). Based on Table 8, this specimen is the strongest one. The 3-phase diagram is shown in Fig. 4.

Zone 2 is the one with stir zone and has a low density of Zn, within which Al has decreased based on EDS element analysis. Element analysis of zone 2 has been indicated in Table 7. By studying the 3-phase diagram, it is clear that there exists solid solution and 3-phase eutectic compounds which cause low possibility of intermetallic compound formations. Figure 9c shows magnifying zone 2 and element analysis zones.

Zone 3 is an interface of a possible area for intermetallic compounds(Firouzdor and Kou, 2010). Considering SEM magnified Fig. 9d and point analysis shown in Table 7, different points are investigated. Point E is placed in the solid solution area and 3-phase eutectic compound based on EDS element-point analysis. Point F which is close to Mg zone is toward Mg solid solution and 3-phase eutectic compound in the diagram. Point D which is at the center of interface is located in an area with constant $MgZn_2$ (Liu *et al*., 2012, 2013; Zhang *et al*., 2015).

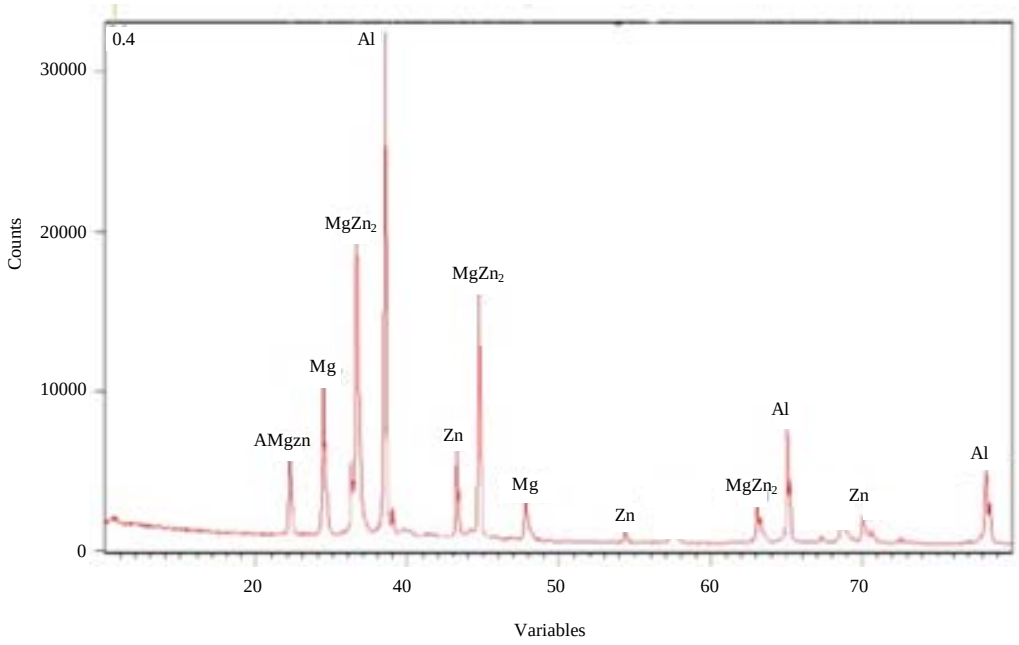

Fig. 8: XRD from joint zone with a 200 μ interlayer

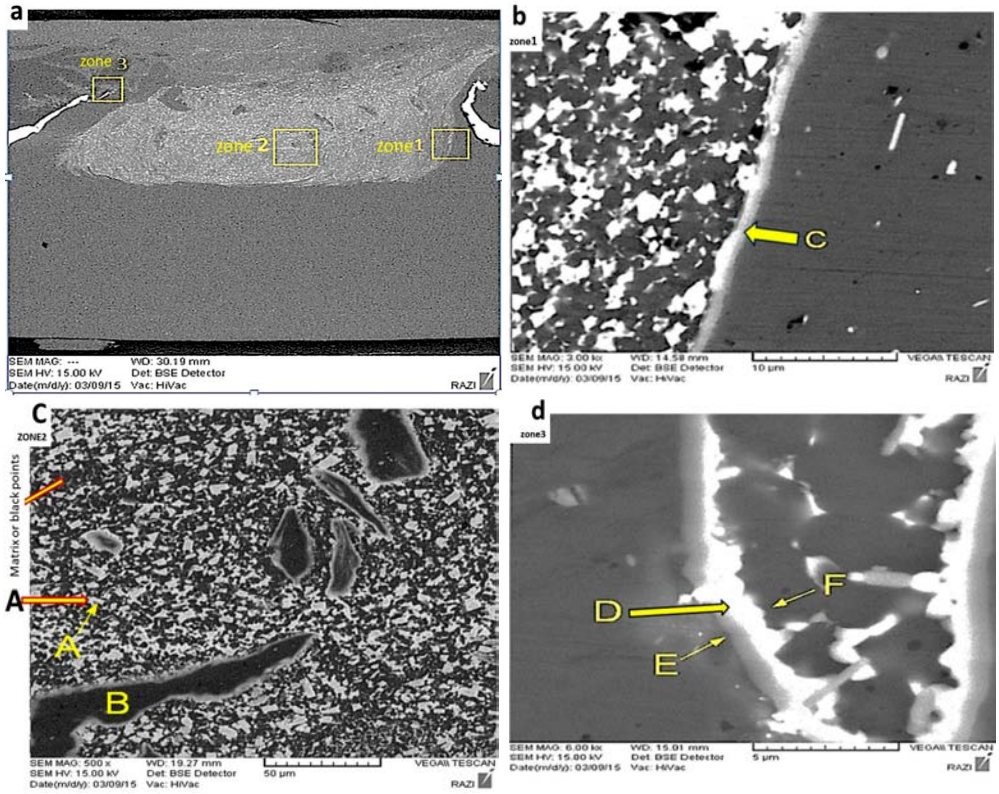

Fig. 9: a) SEM image of welding zone and analyzed area with 100 μ-interlayer; b) Magnifying of zone 1 in Fig. 9a and point-to-point element analysis areas; c) Magnifying of zone 2; d) Magnifying of zone 3 and details

Table 7: Element analysis of zones 1-3 of welding 100 μ-interlayer

Test zones/focus point of the microscope	Al atomic (%)	Mg atomic (%)	Zn atomic (%)
Zone 1			
C	81.34	15.68	2.980
Zone 2			
A	16.88	56.39	26.73
B	98.18	1.240	0.580
Matrix (black point)	3.510	92.56	3.930
Zone 3			
D	51.03	28.13	20.84
E	12.68	51.61	34.65
F	4.180	83.03	12.79

Table 8: Result of shear tensile strength test by interlayer

Thickness of interlayer (μ)	Height of pin (mm)	Travel speed (mm min^{-1})	Rotational speed rpm	Weld strength (N/mm^2)	Imposed force (N)
100	2.6	40	1600	76	2280
200	2.6	40	1600	70	2100
400	2.6	40	1600	63	1910

Based on microscopic investigation of interface, intermetallic compound is likely to be observed. But here, the intermetallic compound contiguous and has a trace of Mg in some points. This fact can affect welding mechanical properties positively (Yamamoto *et al*., 2009) (Fig. 10).

By investigating XRD of welding zone in a 100 μ-interlayer specimen, it is obvious that $MgZn_2$ as an intermetallic compound exists in the welding zone and joint interface. We can observe Al in the stir zone which causes low possibility of intermetallic compound formation. Figure 11 indicates the result of XRD of a 100 μ-interlayer specimen.

As the minimum temperature in the FSW process is approximately around 430, 450 and 460°C (Chen and Nakata, 2008; Firouzdor and Kou, 2010; Yamamoto *et al*., 2009) and at last Zn has been found molten (Fig. 12), so melting point is 419.5°C. As a result, in this research, the temperature is >420°C. The eutectic transformation temperature for formation of intermetallic compound is 350, 360 and 390°C (Zhao and Zhang, 2008; Liu *et al*., 2009; Zhang *et al*., 2015) and this fact can be find out by referring to the 2-phase diagram and observing eutectic transformation temperature. Also, partial melting in Mg/Al and its effect on the formation of solidified, eutectic and intermetallic structures is reported (Firouzdor and Kou, 2010; Yamamoto *et al*., 2009; Derazkola *et al*., 2015; Nandan *et al*., 2006; Eiyasi *et al*., 2015; Frigaard *et al*., 2001). Here, Zn is in molten state,

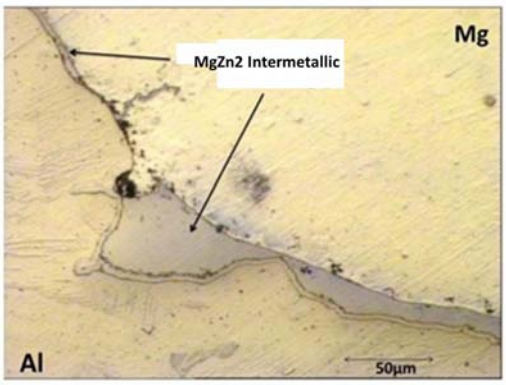

Fig. 10: Microscopic image of joint interface with 100 µ-interlayer

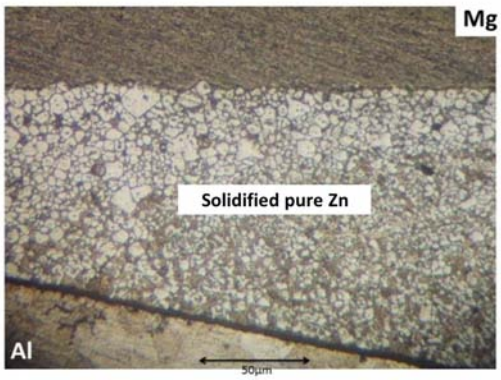

Fig. 11: Microscopic Image of solidified Zn in the interface of joint with 200 µ-interlayer

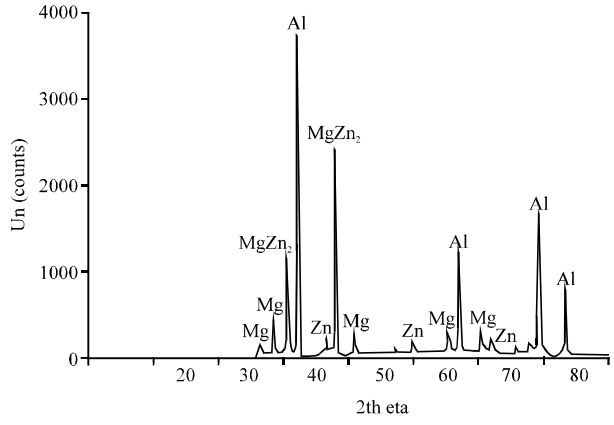

Fig. 12: XRD from a 100 µ-interlayer specimen

so, there is a possibility of the formation of solidified, eutectic and intermetallic structures in welding zone. The presence of $MgZn_2$ in the welding zone can be proved by XRD results. These results has been shown in Fig. 6, 8 and 11:

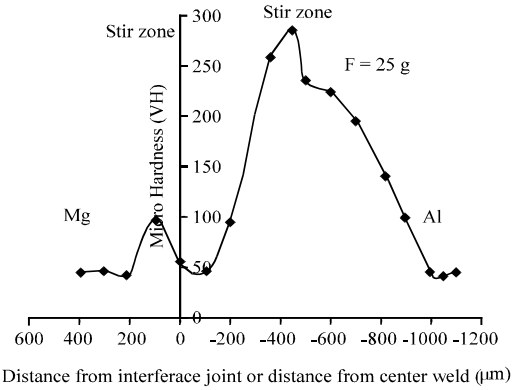

Fig. 13: Hardness changes chart in interface of joint

At 350°C $L \rightarrow Mgzn_2$

Tensile strength: Based on the investigations, Zn interlayer causes an increase in theweld shear tensile strength. Even by decreasing the thickness of Zn interlayer, the weld tensile strength increases. So, it can be concluded that as we decrease the thickness of Zn interlayer, Zn level has decreased in the welding zone. By investigating the 3-phase diagram, we observe the low possibility of $MgZn_2$ formation. So, by decreasing Zn thickness, weld tensile strength will increase. The 100 µ-interlayer tolerate 2.28 KN which was 1.8 for the specimen without interlayer (Chen and Nakata, 2008, 2009). Weld tensile strength depends on the shape and thickness of intermetallic compounds, e.g., an increase in constant intermetallic compound and its thickness will decrease weld tensile strength (Firouzdor and Kou, 2009; Chen and Nakata, 2009; Sarvari and Divandari, 2015; Wang *et al*., 2013; Sato *et al*., 2004; Yamamoto *et al*., 2009).

Micro hardness changes in joint: Figure 13 shows the hardness changes in interface of joint. As it is shown, the amount of hardness fluctuated a lot with a distance of 0.5 mm from Al/Mg interface of joint(weld center). This happens as a result of complex structure of stir zoneand intermetallic compound formation. Often, in Al/Mg joint, hardness in mixing area (stir zone) is at the top because of intermetallic compound in the weld interface joint (Mofid *et al*., 2012; Yan *et al*., 2010).

By the help of Zn interlayer, there exists no trace of intermetallic compound such as Al_3Mg_2, $Al_{12}Mg_{17}$. $MgZn_2$ intermetallic compound has been observed which is not continuous in 100 µ-interlayer specimen. In stir zone, besides complex structure composed of Al and Mg layer, there is a possibility of the presence of solidification and eutectic structures of Al, Mg and Zn.

Welding with 400 μ-interlayer causes many holes at the bottom of the stir zone. This is not the case for the 200 and 100 μ. Al density in the stir zone with 200 and 400 μ-interlayers is lower than that of 100 μ. Weld tensile strength has been increased when interlayer is applied. By decreasing interlayer thickness, weld tensile strength will increase.

CONCLUSION

The results show that with the presence of Zn layer, the eutectic compound has been formed within the weld zone and the intermetallic $MgZn_2$ has been produced. So, weld strength increased by the Zn interlayer (Zhang *et al*., 2015). In 2007 and 2008, Liu and co investigated the solder joint of Al/Mg with Zn filler metal. As a result, a compound of Al/Zn solid solution caused the joint without intermetallic formations which was strong also (Liu *et al*., 2008, 2007).

REFERENCES

Chen, Y.C. and K. Nakata, 2008. Friction stir lap joining aluminum and magnesium alloys. Scripta Mater., 58: 433-436.

Chen, Y.C. and K. Nakata, 2009. Friction stir lap welding of magnesium alloy and zinc-coated steel. Mater. Trans., 50: 2598-2603.

Derazkola, H.A., M. Habibnia and H.J. Aval, 2015. Study on frictional heat behavior and material flow during friction stir welding of AA1100 aluminum alloy. Modares Mech. Eng., 14: 251-261.

Elias, M., C. Aqajani and H.M. Zadeh, 2015. Effects of friction stir welding parameters on mechanical quality of AA1100 aluminum alloy to A441 AISI steel joint. Mech. Eng. Lecturer, 15: 379-390.

Elyasi, M., H.A. Derazkola and M. Hoseinzadeh, 2015. Study on joint zone microstructure evolution and hardness in friction stir welding of AA1100 aluminum alloy to A441 AISI steel. Modares Mech. Eng., 14: 97-107.

Firouzdor, V. and S. Kou, 2009. Al-to-Mg friction stir welding: Effect of positions of Al and Mg with respect to the welding tool. Weld. J., 88: 213-224.

Firouzdor, V. and S. Kou, 2010. Formation of liquid and intermetallics in Al-to-Mg friction stir welding. Metall. Mater. Trans. A, 41: 3238-3251.

Frigaard, O., O. Grong and O.T. Midling, 2001. A process model for friction stir welding of age hardening aluminum alloys. Metall. Mater. Trans. A, 32: 1189-1200.

Kostka, A., R.S. Coelho, D.J. Santos and A.R. Pyzalla, 2009. Microstructure of friction stir welding of Aluminium alloy to magnesium alloy. Scripta Mater., 60: 953-956.

Liu, F., D. Ren and L. Liu, 2013. Effect of Al foils interlayer on microstructures and mechanical properties of Mg-Al butt joints welded by gas tungsten arc welding filling with Zn filler metal. Mater. Des., 46: 419-425.

Liu, F., Z. Zhang and L. Liu, 2012. Microstructure evolution of Al-Mg but joints welded by gas tungsten arc with Zn filler metal. Mater. Charact., 69: 84-89.

Liu, L. and S. Liu, 2006. Mictostructure of laser-tig hybrid welds of dissimilar Mg alloy and Al alloy with Ce as interlayer. Scr. Mater., 55: 383-386.

Liu, L., J. Tan and X. Liu, 2007. Reactive brazing of Al alloy to Mg alloy using zinc-based brazing alloy. Mater. Lett., 61: 2373-2377.

Liu, L.M., J.H. Tan, L.M. Zhao and X.J. Liu, 2008. The relationship between microstructure and properties of Mg-Al brazed joints using Zn filler metal. Mater. Charact., 59: 479-483.

Liu, L.M., L.M. Zhao and R.Z. Xu, 2009. Effect of interlayer composition on the microstructure and strength of diffusion bonded Mg-Al joint. Mater. Des., 30: 4548-4551.

Mclean, A.A., Powell G.L.F., Brown, L.H. and V.M. Linton, 2003. Firiction stir welding of magnesium alloy AZ31B to aluminium alloy 5083. Sci. Technol. Weld. Joining, 8: 462-464.

Mishra, R.S. and Z.Y. Ma, 2005. Friction stir welding and processing. Mater. Sci. Eng.: R: Rep., 50: 1-78.

Mofid, M.A., A.A. Zadeh and F.M. Ghaini, 2012. The effect of water cooling during dissimilar friction stir welding of Al alloy to Mg alloy. Mater. Des., 36: 161-167.

Nandan, R., G.G. Roy and T. Debroy, 2006. Numerical simulation of three-dimensional heat transfer and plastic flow during friction stir welding. Metall. Mater. Trans. A, 37: 1247-1259.

Sarvari, M. and M. Divandari, 2015. Melt behavior and shrinkage force effect of Al melt in Al-Mg bimetal casted via centrifugal casting. Modares Mech. Eng., 15: 131-138.

Sato, Y.S., S.H.C. Park, M. Michiuchi and H. Kokawa, 2004. Constitutional liquation during dissimilar friction stir welding of Al and Mg alloys. Scripta Mater., 50: 1233-1236.

Szymanski, R.T., S.K. Chimbli, M.T. Hall and Y.L. Chen, 2010. Friction Stir Welding of Dissimilar Metals. Patent Publication, USA.,.

Venkateswaran, P. and A.P. Reynolds, 2012. Factors affecting the properties of friction stir welds between aluminum and magnesium alloys. Mater. Sci. Eng. A, 545: 26-37.

Wang, H.Y., Z.D. Zhang and L.M. Liu, 2013. The effect of galvanized iron interlayer on the intermetallics in the laser weld bonding of Mg to Al fusion zone. J. Mater. Eng. Perform., 22: 351-357.

Yamamoto, N., J. Liao, S. Watanabe and K. Nakata, 2009. Effect of intermetallic compound layer on tensile strength of dissimilar friction-stir weld of a high strength Mg alloy and Al alloy. Mater. Trans., 50: 2833-2838.

Yan, Y., D.T. Zhang, C. Qiu and W. Zhang, 2010. Dissimilar friction stir welding between 5052 aluminum alloy and AZ31 magnesium alloy. Transition Nonferrous Metal Soc. China, 20: s619-s623.

Zhang, H.T. and J.Q. Song, 2011. Microstructural evolution of aluminum-magnesium lap joints welded using MIG process with zinc foil as an interlayer. Mater. Lett., 65: 3292-3294.

Zhang, Y., Z. Luo, Y. Li, Z. Liu and Z. Huang, 2015. Microstructure characterization and tensile properties of Mg-Al dissimilar joints manufactured by thermo-compensated resistance spot welding with Zn interlayer. Mater. Des., 75: 166-173.

Zhao, L.M. and Z.D. Zhang, 2008. Effect of Zn alloy interlayer on interface microstructure and strength of diffusion-bonded Mg-Al joints. Scripta Mater., 58: 283-286.